ELSEVIER

15 June 1998

PHYSICS LETTERS A

Physics Letters A 243 (1998) 60–65

Extreme low aspect ratio stellarators

Paul E. Moroz

Center for Plasma Theory and Computation, Department of Engineering Physics, University of Wisconsin-Madison, Madison, WI 53706, USA

Received 10 December 1997; accepted for publication 5 March 1998
Communicated by M. Porkolab

Abstract

A novel class of stellarator configurations with unique and advanced characteristics is proposed. It features extreme low plasma aspect ratios (down to $A \approx 1$), a simple coil system having a helical center post, extremely high β equilibria ($\beta_0 \sim 90\%$, $\beta \sim 20\%$ is demonstrated) assisted by a strong positive bootstrap current, improved particle transport caused by the absence of an outboard helical ripple, and a natural divertor. The helical center post can be a single helix or may consist of a few helices. © 1998 Elsevier Science B.V.

PACS: 52.55.Hc

Stellarators are normally large aspect ratio devices (the aspect ratio, A, is the ratio of the average major radius to the average minor radius for the last closed flux surface), with A usually being in the range of 7–10 (see, for example, Refs. [1–4]). The lowest-A stellarators ever built have $A \approx 5$ [5–7].

Relatively recently, the spherical stellarator (SS) concept [8,9] (called so in analogy with the spherical Tokamak (ST) concept [10,11]) was proposed. The main characteristics of a SS, included in the definition of this novel class of magnetic confinement devices, constitute the following unique combination: (i) very low plasma aspect ratio stellarator device, $A \leqslant 3.5$, (ii) high β limits, well above 1–5% typical for traditional stellarators, and (iii) positive and strong plasma current (positive means that the current flows in such a direction that the total rotational transform increases in comparison with its vacuum value, and strong means that its contribution to the total rotational transform is significant). The SS concept includes configurations that, when being scaled to the large size and high-β, feature a positive bootstrap current strong enough [9,12,13] to support the above-mentioned advanced characteristics of the SS, without requiring any external current drive. Improved particle transport and simplicity of the coils are also the goals of the SS approach. For small SS devices which cannot rely on a significant bootstrap current, an ohmic or auxiliary driven current can be used in the corresponding experiments. The definition of the SS concept does not include specifications for the particular optimization procedure leading to improved particle transport and enhanced high β limits, because different procedures are possible and different configurations can be obtained within the SS concept.

A few SS configurations, differing principally in the types of simple coils to be used, have been analyzed [8,9,12–16]. Coil configurations with a straight center post, planar coils, and outboard stellarator windings have been considered. More complicated coils

PII S0375-9601(98)00215-1

combining a few different types were considered as well. Research on SS grew significantly during the last year and involves a number of institutions. Researchers at ORNL are investigating a closely related concept, the SMARTH (small aspect ratio toroidal hybrid) [12,17–21]. Their research is focused on the so-called quasi-omnigenous approach and J^* optimization of particle transport. A different case of SS optimization regarding the particle transport, based on the quasi-axisymmetric approach [22], was initiated recently by the PPPL team [23–25]. The aspect ratios for the configurations presently considered by the ORNL and PPPL teams are $A \approx 2.5$–3.5. Some other institutions have also become involved in this kind of low aspect ratio stellarator research.

The present paper introduces a novel class of stellarators. They have a few very unique and advantageous characteristics not only in comparison with traditional large aspect ratio stellarators but also in comparison with the SS configurations mentioned above. These are the extreme low aspect ratio stellarators (ELARS). As a particular example, the ELARS configurations considered here feature the helical center post consisting of a single helix or a few helices, and thus can be called also the helical post stellarators (HPS). The main advanced features that we include in the definition of this novel class of stellarators consist of the following combination of unique characteristics: (i) extremely low plasma aspect ratio, $A \leqslant 1.5$, (ii) simple coil system featuring a helical center post, (iii) extremely high β limits assisted by a strong positive bootstrap current, and (iv) improved particle transport. Actually, the plasma aspect ratios of the configurations discussed in this paper are even lower, $A \leqslant 1.2$, although some interesting cases with $A \leqslant 1.5$ have been found as well.

In this paper we briefly introduce the ELARS configurations and demonstrate the above-mentioned advantages. We present a few results for a single-helix stellarator (SHS), double-helix stellarator (DHS), and triple-helix stellarator (THS). In the configurations considered, the helical center post is the only helical element of the coil system responsible for the stellarator characteristics. More complicated configurations combining the helical center post with the other helical elements of the coil system are possible but are beyond the cope of the present paper.

To our knowledge, the ELARS configurations presented are unique among all previously considered stellarators, including the SS analyzed so far, in that the magnetic field ripple is located practically entirely on the inboard of the torus. This improves particle transport according to the theory [26,27]. This method of transport optimization can probably be called generalized σ-optimization or s-optimization, because it generalizes an approach to σ-optimization [26] or s-optimization [27].

The coil systems of the ELARS considered are shown in Figs. 1a–c. The outboard parts of the toroidal field (TF) coils and the system of the poloidal field (PF) rings are the same as in a typical ST. The difference, however, is in the helical center post, and the three cases presented correspond to SHS (a), DHS (b), and THS (c). The perspective view of the last closed vacuum flux surface together with the coil system for these three configurations is shown correspondingly in Figs. 2a–c. The PF rings are actually used in these calculations only for the case of a SHS to push the plasma further inside and reduce the outboard magnetic ripple. It is important to mention that generally vacuum flux surfaces with large enclosed volumes and a significant rotational transform can be obtained without PF rings for all of the ELARS configurations considered. However, the PF rings are necessary for obtaining high-β MHD equilibria.

The HPS configurations feature extremely low aspect ratios: $A \approx 1$ for SHS, $A \approx 1.1$ for the DHS, and $A \approx 1.2$ for the THS. Also, the SHS is the stellarator configuration that has only a single toroidal period, $N = 1$, which is very unusual. To our knowledge, there were only two other stellarator configurations with $N = 1$ proposed and briefly discussed in the past: the Cleftron [28] and the ultra-simple stellarator [29]. Both these configurations had straight center columns. The Cleftron's coil system consists of a single outboard helical winding connecting the bottom and top parts of the straight center column and making one turn around it, while the ultra-simple stellarator has two interconnected planar coils: a small circular and a very large rectangular. These $N = 1$ configurations, however, do not feature many attractive characteristics of the SHS.

The area around the center helical post is not accessible to plasma particles as the field lines become opened there and form a natural divertor. To demonstrate this feature, Fig. 3 shows the field line traces for

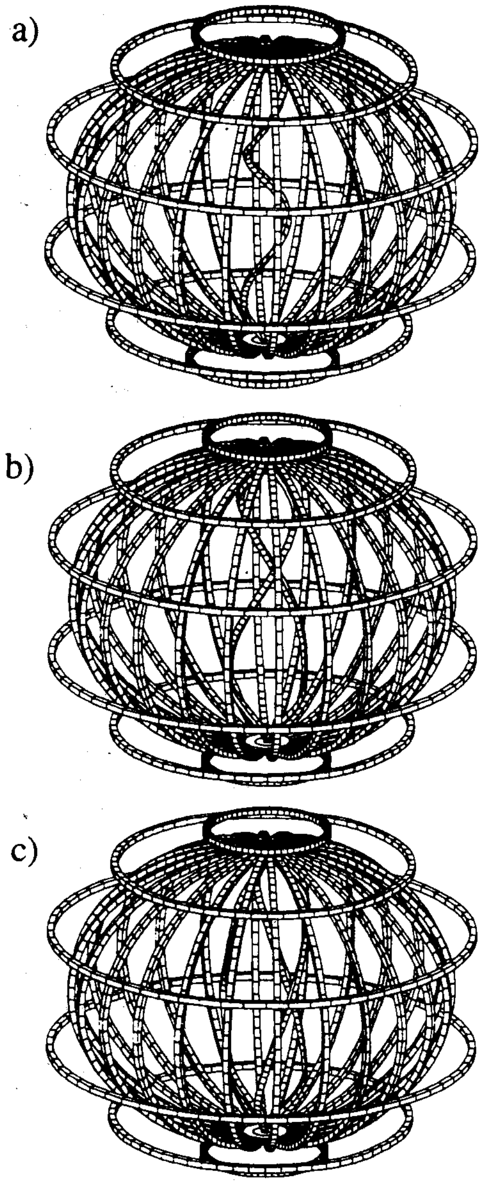

Fig. 1. The coil systems of the SHS (a), DHS (b), and THS (c).

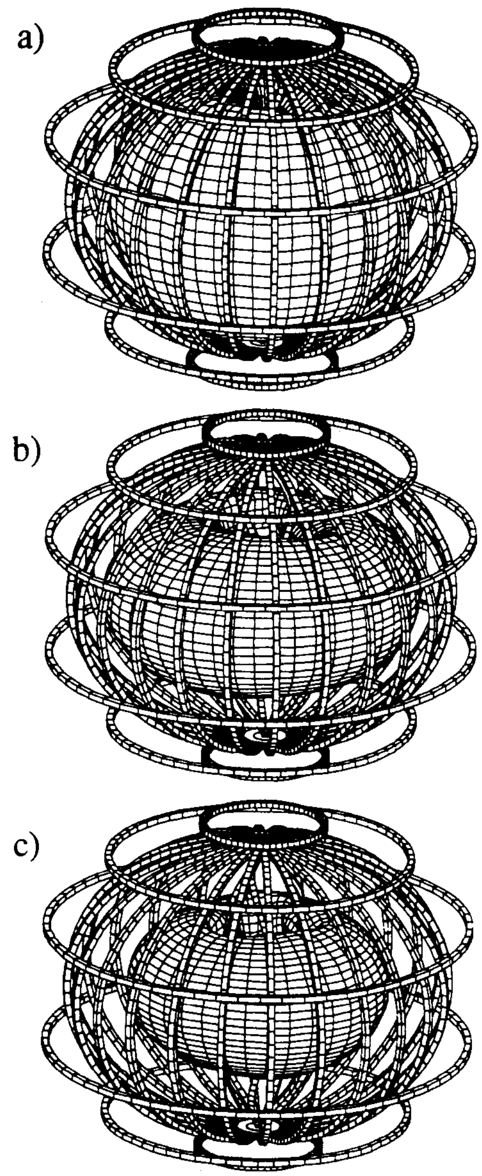

Fig. 2. Perspective view on the last closed vacuum flux surfaces in the SHS (a), DHS (b), and THS (c).

a SHS without PF rings. The traces of the two opened field lines near the center post are shown by the dashed curves.

To further demonstrate the general advantages of the ELARS concept, we present here just a few results of the calculations obtained with the 3D MHD equilibrium code, VMEC [30], running in free-boundary mode, 3D field line tracing code, UBFIELD [31], and 3D bootstrap current code, BOOTSJ [32,9]. A much more detailed analysis will be given in separate publications [33,34].

A typical radial profile of the vacuum rotational transform for an ELARS is demonstrated in Fig. 4, where a solid curve corresponds to the SHS case without the PF rings and a dashed curve to that with the finite currents in the PF rings. As one can see, the vac-

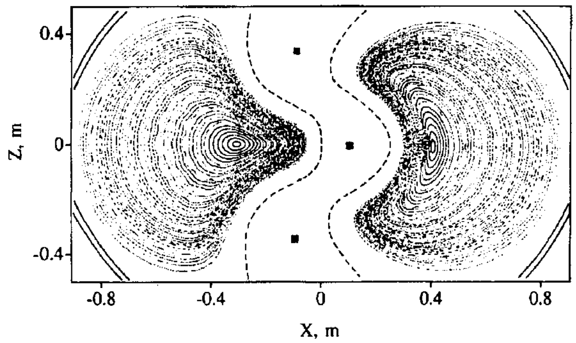

Fig. 3. Poincaré puncture plots for closed vacuum flux surfaces in the X–Z cross-section of a SHS without PF rings. The dashed curves demonstrate the geometry of opened field lines around the helical post. Cross-sections of the coils are shown as well.

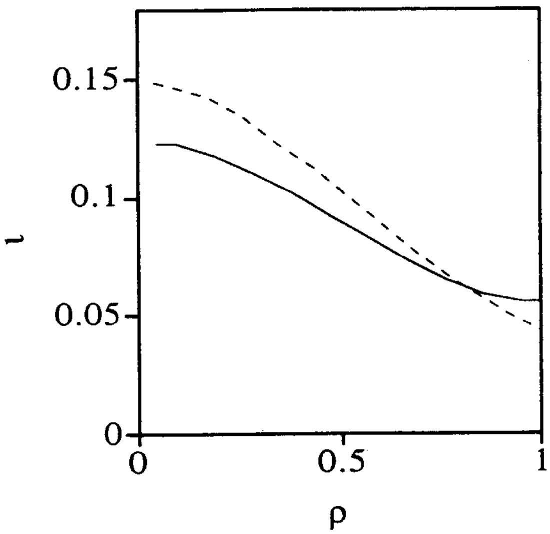

Fig. 4. Radial dependence of the rotational transform for the SHS without PF rings (solid curve) and with PF rings (dashed curve).

uum rotational transform is a decreasing function of minor radius, similar to that in a traditional Tokamak or in the previously considered SS devices.

To demonstrate the improved particle transport characteristics in the ELARS, Fig. 5 shows the ratio S/S_0 for the same SHS configurations as Fig. 4. Here, the parameter S [27] is proportional to the neoclassical flux, and S_0 corresponds to the similar but non-optimized case when the helical ripple is distributed evenly on each flux surface. Improvement by a factor of 2 to 5 depending on the minor radius is clearly seen.

A typical $|B|$ distribution along the flux surfaces of an ELARS is shown in Fig. 6, where the case of

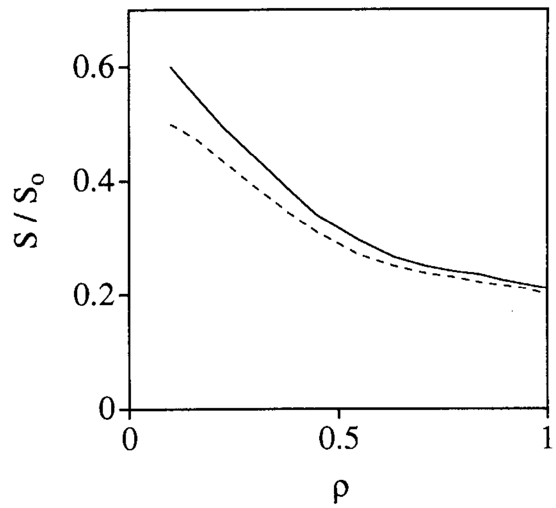

Fig. 5. Radial dependence of S/S_0 for the SHS without PF rings (solid curve) and with PF rings (dashed curve).

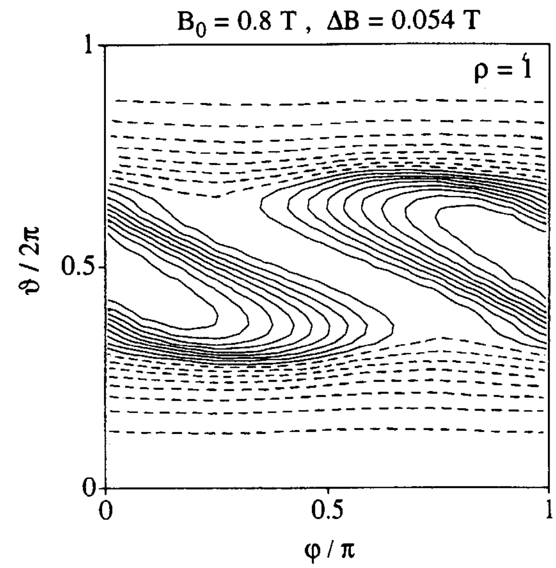

Fig. 6. $|B|$ distribution on the last closed vacuum flux surface of the DHS. Solid contours are for $B \geqslant B_0$, dashed for $B < B_0$. ΔB is the difference between adjacent contours.

vacuum DHS field is presented and the last flux surface is considered. All ELARS discussed here have a common feature in the $|B|$ distribution: the quasi-helical symmetry on the inboard of the torus and quasi-toroidal symmetry on the outboard.

To demonstrate the extremely high β characteristics of the ELARS, the left column of Fig. 7 shows the flux surfaces for the MHD plasma equilibrium in a

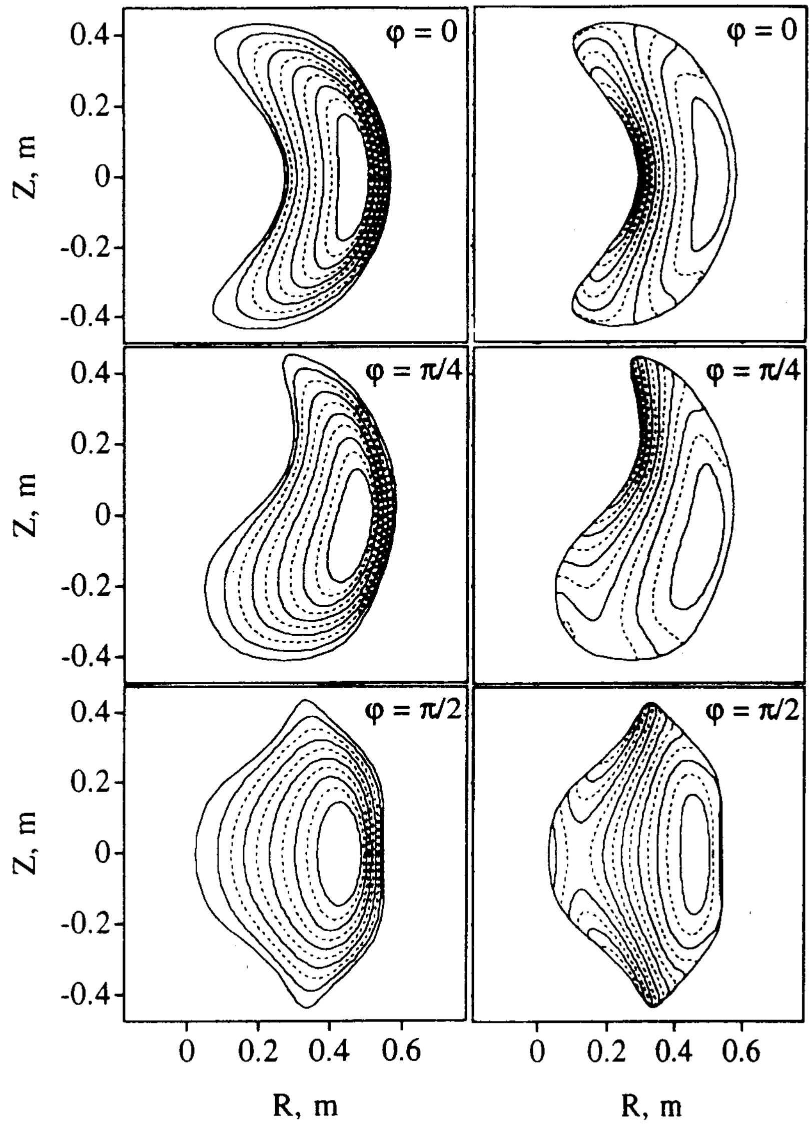

Fig. 7. High β ($\beta_0 = 86\%$, $\beta = 20\%$) MHD equilibrium in the DHS with the self-consistent bootstrap current. Flux surfaces (left column) and contours of $|B|$ (right column) are shown.

DHS at the central $\beta_0 = 86\%$ and the volume average $\beta = 20\%$. This equilibrium corresponds to a toroidal flux, $\Phi \approx 0.2$ Wb, a self-consistent bootstrap current, $I_{bs} \approx 300$ kA, and the total rotational transform increasing from about $\iota \approx 0.15$ near the magnetic axis to $\iota \approx 0.3$ at the plasma boundary. Here, $\iota = 1/q$, q being the safety factor. Such an increasing of ι with minor radius might be advantageous for suppression of magnetic islands at high β [35], which otherwise might grow with increasing plasma pressure. The contours of $|B|$ for the same three main cross-sections are shown in the right column of Fig. 7. The partial omnigeneity [36] (for the ideal case, the $|B|$ contours coincide with the flux surfaces) is clear seen. This is advantageous for the further improvement of particle transport in the ELARS. The location of the minimum $|B|$ near the magnetic axis in all cross-sections causes the radial β profile to be much more peaked than the corresponding pressure profile.

In conclusion, a novel and very unusual class of stellarators, the ELARS with the helical center post, was introduced and particular examples for the SHS, DHS, and THS configurations were presented. Many unique characteristics such as extremely low plasma aspect ratios, extremely high β MHD equilibria, a natural divertor protecting the helical post, and improved particle transport were demonstrated. Although the magnetic field in the ELARS does not generally correspond to toroidal symmetry or omnigeneity, the particle transport is improved (via generalized σ-optimization).

The ELARS coil system can be built relatively easily from the corresponding ST configuration by replacing the straight center post of a ST with a helical center post, or possibly by winding a helix around the straight center post of a ST. The main goal of such a transformation from an ST to ELARS is to obtain a device with advanced characteristics which can operate in a steady-state regime for any given plasma pressure below some high limit.

This paper introduces the ELARS concept and briefly demonstrates its promising characteristics. Significant additional research and optimization are necessary before the final conclusion on advantages of this concept for controlled fusion can be made.

While this paper was under review, a few new results have been obtained for the ELARS considered, which we would like to mention here. Among the most important ones are probably the results of Monte Carlo transport simulations [33,34] which confirmed improved particle confinement in the ELARS and demonstrated the diffusion coefficient values close to that in an equivalent Tokamak.

The author is thankful to S.P. Hirshman for using the 3D MHD equilibrium code, VMEC. He also would like to acknowledge useful discussions of various related questions with S.P. Hirshman, D.B. Batchelor, D.A. Spong and J.D. Callen. This work was supported in part by the U.S. DOE Grant No. DE-FG02-97ER54395.

References

[1] J.H. Harris et al., Fus. Tech. 17 (1990) 51.
[2] J. Sapper et al., Fus. Tech. 17 (1990) 62.
[3] C. Beidler et al., Fus. Tech. 17 (1990) 148.
[4] M. Wakatani et al., Pl. Phys. Contr. Fus. 38 (1996) 937.
[5] K. Nishimura et al., Fus. Tech. 17 (1990) 86.
[6] M.G. Shats et al., Phys. Rev. Lett. 77 (1996) 4190.
[7] S.F. Knowlton et al., J. Fus. Energy 12 (1993) 261.
[8] P.E. Moroz, Phys. Rev. Lett. 77 (1996) 651.
[9] P.E. Moroz, Phys. Plasmas 3 (1996) 3055.
[10] M. Peng et al., Nucl. Fusion 26 (1986) 576.
[11] A. Sykes, Pl. Phys. Contr. Fus. 36 (1994) B 93.
[12] P.E. Moroz et al., Fus. Tech. 30 (1996) 1347.
[13] P.E. Moroz, Stellarator News 48 (1996) 2.
[14] P.E. Moroz, Pl. Phys. Contr. Fus. 39 (1997) 1841.
[15] P.E. Moroz, Plasma Phys. Rep. 23 (1997) 502.
[16] P.E. Moroz, Nucl. Fusion 37 (1997) 1045.
[17] B.A. Carreras et al., Rep. ORNL/TM-13252 (August 1996).
[18] D.A. Spong et al., Plasma Phys. Rep. 23 (1997) 483.
[19] D.A. Spong et al., Stellarator News 52 (1997) 1.
[20] D.W. Ross et al., Plasma Phys. Rep. 23 (1997) 492.
[21] S.P. Hirshman et al., Bull. Amer. Phys. Soc. 42 (1997) 1912.
[22] P.R. Garabedian, Phys. Plasmas 3 (1996) 2483.
[23] A. Reiman et al., Bull. Amer. Phys. Soc. 42 (1997) 1913.
[24] M.C. Zarnstorff et al., Bull. Amer. Phys. Soc. 42 (1997) 1914.
[25] R.J. Goldston, IAEA Tech. Comm. Meet., Pleasanton (October 1997).
[26] H.E. Mynick et al., Phys. Rev. Lett. 48 (1982) 322.
[27] K.C. Shaing et al., Phys. Fluids 28 (1983) 2136.
[28] T. Ohkawa, 3rd Stellarator Workshop, Vol. 1 (Moscow, 1981), p. 111.
[29] T.N. Todd, Plasma Phys. Contr. Fusion 32 (1990) 459.
[30] S.P. Hirshman et al., Comp. Phys. Comm. 43 (1986) 143.
[31] P.E. Moroz, Phys. Plasmas 2 (1995) 4269.
[32] K.C. Shaing et al., Phys. Fluids B 1 (1989) 1663.
[33] P.E. Moroz, Helical Post Stellarator, to be published in Plasma Phys. Contr. Fusion (1998).
[34] P.E. Moroz, Novel Stellarator Configuration with Double-Helix Center Post, to be published in Nucl. Fusion (1998).
[35] R.J. Goldston, Sherwood '97 Fus. Theor. Conf., Madison, 2C26 (1997).
[36] L.S. Hall et al., Phys. Fluids 18 (1975) 552.